Eur Biophys J (1991) 20:177–182

European Biophysics Journal

The quenching of tryptophan fluorescence by protonated and unprotonated imidazole

K. Willaert and Y. Engelborghs

University of Leuven, Laboratory of Chemical and Biological Dynamics, Celestijnenlaan 200 D, B-3001 Leuven, Belgium

Received February 13, 1991/Accepted in revised form June 7, 1991

Abstract. The fluorescence life-time of N-acetyl-tryptophan-amide (NATA) was measured by multifrequency phase fluorometry, in the presence of increasing concentrations of imidazole. Two pH values were tested, pH 4.5 where imidazole is fully protonated and pH 9.0 where it is fully unprotonated. At both pH values, the inverse life-time increases in a non-linear way with the imidazole concentration, showing that imidazole is not a high efficiency collisional quencher. The data can be analysed in terms of the formation of a complex with a reduced fluorescence life-time. The rate constants for association (at 25 °C) are around $5\,(\pm 0.2)\times 10^9\ M^{-1}\ s^{-1}$ and are thus diffusion controlled. The association equilibrium constant is strongly pH dependent and is much higher than the expected value of $0.4\ M^{-1}$ for a collisional complex. The intrinsic fluorescence life-time of the complex is 1.56 ($\pm$0.02) ns at pH 9.0 and 1.82 ($\pm$0.03) ns at pH 4.5, as compared to 2.37 ($\pm$0.03) ns for free NATA at pH 9.0 and 2.83 ($\pm$0.05) at pH 4.5 (all at $I=0.34$). This means that at both pH values the fluorescence life-time of NATA in the complex is reduced to 61 ($\pm$0.5)% of its value in the free state. Despite this, the protonated form of imidazole is a better quencher at low concentrations, owing to a longer residence-time of the complex. At high viscosity the association equilibration is too slow and the system is described by two life-times. The quenching effect of *His*-18 on the fluorescence of the proximal *Trp*-94 of barnase (Loewenthal et al. 1991, Willaert et al. 1991) is discussed in terms of these findings.

Key words: Fluorescence – Tryptophan – Life-time – Phase fluorometry – Imidazole – Histidine

Introduction

Fluorescence spectroscopy (stopped flow) has been used extensively for the study of the time dependence of conformational changes in proteins. The conformational changes can be subtle, for example those occurring upon interaction with other molecules (effectors, substrates, inhibitors, nucleic acids etc.) or upon a change in the solution conditions (pH, ionic strength, hydrophobicity), or more dramatic upon protein unfolding and refolding. Usually the fluorescence changes are only used as a pragmatic tool to detect the changes, but an interpretation at the molecular level is not available. This will become possible when the factors in the protein environment which determine the fluorescent properties of the probe in use (e.g. tryptophan) are known. A detailed study of single tryptophan proteins and their mutants should allow the characterisation of the salient features. The same is true for multi-tryptophan proteins provided the fluorescent life-times can be resolved and attributed to individual tryptophans, and a correlation with their environment can be made. A nice example is lactate dehydrogenase from *Bacillus stearothermophilus*, where the life-times could be assigned to individual tryptophans but no correlation with the protein environment could be made (Waldman et al. 1987).

The multiple life-times found for *Trp* in solution, as distinct from the single life-time found for NATA, indicate the importance of the presence of $-COO^-$ and $-NH_3^+$ groups in close proximity to the indole group (Szabo and Rayner 1980a, b). Although NATA is the best model compound for a *Trp* residue in a protein, the same groups can be present as side chains from other amino acids or from the terminal amino acid residues. Other side chains may also be of importance. Here we studied the effect of the protonated and unprotonated imidazole group, the side chain of histidine. This work is inspired by the study of the pH dependence of the steady state fluorescence of barnase. This pH dependent fluorescence shows a pKa corresponding to *His*-18 (Loewenthal et al. 1991). A multifrequency phase fluorometric study (Willaert et al. 1991) revealed that the life-time of *Trp*-94 was influenced by the presence of this residue. Here we studied the fluorescence life-time of NATA in the presence of increasing concentrations of imidazole, in the protonated and unprotonated

Offprint requests to: Y. Engelborghs

state. We observed a non-linear increase of the inverse life-time, pointing to the appearance of a fast parallel decay pathway through the formation of an initial collision complex with the excited state and the subsequent decay of the complex to the ground state. The pH dependence of the effect brings new insight in the pH dependence of the tryptophan fluorescence of barnase.

Material and methods

NATA was purchased from Sigma, imidazole from Janssen Chimica and both were analytical grade. Scintillation grade 1,4 diphenylbenzene was obtained from Sigma.

At pH 4.5 acetate buffer was used. Since imidazolium contributes to the ionic strength, it was kept constant with additional NaCl to 0.34 and 0.5 M. At pH 9.0, *Tris* buffer was used at ionic strengths of 0.1 and 0.34.

A fully automatic multifrequency phase fluorometer was built for the determination of fluorescence life-times (Clays et al. 1989). The excitation source consists of a mode-locked cavity-dumped dye laser and a frequency doubler to obtain light of 295 nm. The output is a train of pulses of about 20 ps width and a frequency of 0.4 MHz. Fourier analysis shows that such a periodic function contains the basic frequency of 0.4 MHz and all its harmonics up to several hundreds of GHz. The emission part consists of a monochromator and a fast photomultiplier. For the sample a UV sensitive model Philips XP2020 was used and for the reference an RCA model 1P28. The gain of the PM is modulated with a chosen harmonic plus a small increment of 700 Hz (cross-correlation). The output of the PM is the product of the periodic fluorescence signal and the modulation function. From this product the 700 Hz term is filtered and phase measurements are done at this low frequency. The frequency synthesisers used to drive the mode locker and to modulate the photomultiplier gain are coupled to the same crystal to improve the phase stability. In this way the value of the phase-shift can be read out within a short measurement time (about 14 min), enabling one to collect data at many (50) modulation frequencies. Since the phase shift can be measured with greater accuracy than the demodulation, the time spent for the measurement is fully used for phase measurements. Detailed statistical techniques are used in the data analysis for phase fluorometry. Mean, standard deviation and percentage in the interval $(-2, +2)$ of the weighted residuals are compared with the predicted values of 0, 1 and 95.5 respectively. An additional quality of fit, the so-called Q-value is also calculated (Clays et al. 1989). The autocorrelation function of the weighted residuals and a plot of these residuals as a function of the calculated phase shift are used as additional visual tests in the data analysis. Data reduction is performed on a Micro Vax 2000 minicomputer using a non linear least-squares algorithm (Bevington 1969). Global analysis has been helpful in the resolution of difficult systems with closely spaced life-times and/or small contributions of some components. (The algorithm used is the modified Levenberg-Marquardt algorithm of More et al. 1983.)

The measured quantities for a set of modulation frequencies (ω) are the phase shifts $\phi(\omega)$. These are related to the fluorescence decay in the time domain $I(t)$ by means of the following equations:

$$I(t)=\Sigma_i\, a_i \exp(-t/\tau_i) \tag{1}$$

$I(t)$ is the time dependent intensity, a_i is the amplitude of the fluorescence signal of the component with life-time τ_i.

$$\tan\phi(\omega)=S(\omega)/G(\omega) \tag{2a}$$

where:

$$S(\omega)=\Sigma_i\, f_i \cdot \cos\Phi_i \cdot \sin\Phi_i \tag{2b}$$

$$G(\omega)=\Sigma_i\, f_i \cdot \cos^2\Phi_i. \tag{2c}$$

Furthermore:

$$\cos\Phi_i=1/(1+\omega^2\cdot\tau_i^2) \quad \text{and} \quad \sin\Phi_i=\omega\,\tau_i/(1+\omega^2\cdot\tau_i^2) \tag{2d}$$

$S(\omega)$ and $G(\omega)$ are the sine and cosine Fourier transforms of $I(t)$, and f_i the steady state contribution of the component with phase shift Φ_i ($f_i=a_i\cdot\tau_i$).

Phase measurements were performed at 25 °C in a thermostated cuvette. The excitation wavelength was 295 nm and the emission was monitored at 340 nm. 1,4 diphenylbenzene was used as a reference, with a life-time of 1.04 ns (Desie et al. 1986).

Results and discussion

The result of a typical phase measurement of NATA at 0.03 M imidazole, pH 4.5, $I=0.34$ is shown in Fig. 1. The phase data can be fitted very well with a single life-time, in agreement with other studies on NATA (Szabo and Rayner 1980b). No improvement is obtained when the data are fitted to a sum of two or more life-times. The results of phase measurements and their analysis for a whole set of imidazole concentrations at two pH values, and different ionic strengths, are shown in Figs. 2 and 3. The inverse of the observed life-time (kobs) is plotted versus imidazole (imidazolium) concentration. The non-linearity of the plot proves that imidazole is not an efficient collisional quencher. The following scheme is proposed:

$$\begin{array}{ccc} T^* + Im & \underset{k_{-1}}{\overset{k_1}{\rightleftharpoons}} & T^*\cdot Im \\ ex \;\Big\downarrow\; k_0 & & ex \;\Big\downarrow\; k_2 \\ T + Im & \rightleftharpoons & T\cdot Im \end{array} \tag{3}$$

in which T and T^* symbolize NATA in the ground state and the excited state respectively, Im stands for imidazole, and $T^*\cdot Im$ for the complex. k_1 is the association rate constant of T^* and Im, k_{-1} the dissociation rate constant of the complex, k_0 is the inverse of the fluorescence life-time of NATA and k_2 of the complex $T^*\cdot Im$. Such a scheme leads to the following two rate equations assuming a δ-pulse excitation. This implies irreversible fluorescence decays and allows the neglect of the ground state

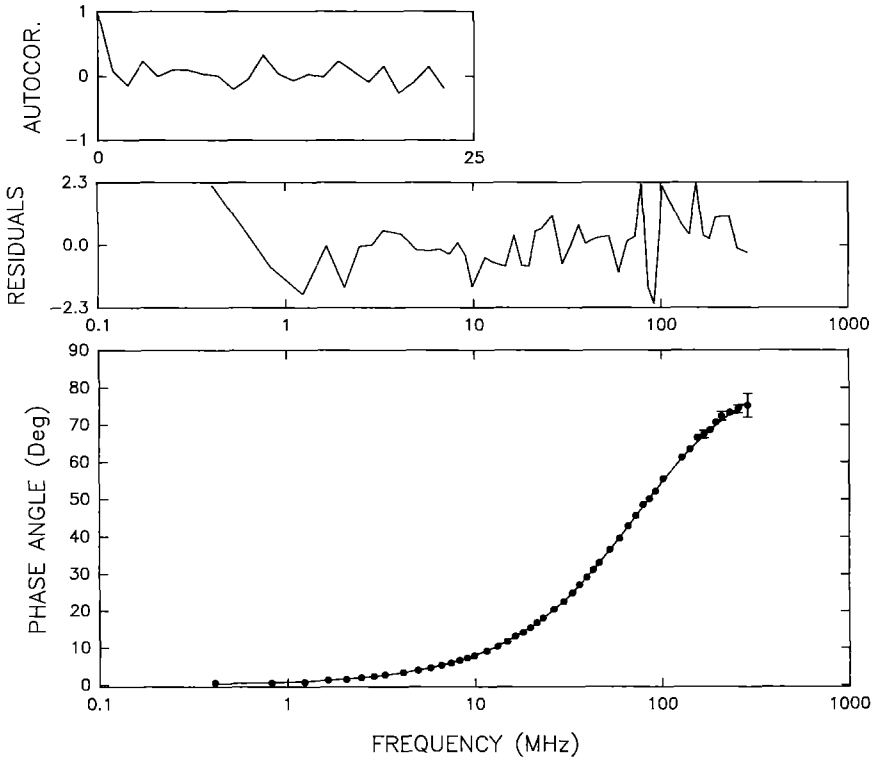

Fig. 1. Phase measurements of NATA at 0.03 M imidazole, pH = 4.5, I = 0.34, and graphical tests incorporated in the data analysis. Plotted are the measured phases and weighted residuals as a function of the frequency and the autocorrelation function of the weighted residuals. The fitting and quality of fit parameters are: reduced chi-square $\chi^2_R = 0.985$; the standard normally distributed $Z_\chi 2 = -0.603$; quality parameter $Q = 0.60$; single life-time $\tau = 2.237 \pm 0.003$ ns

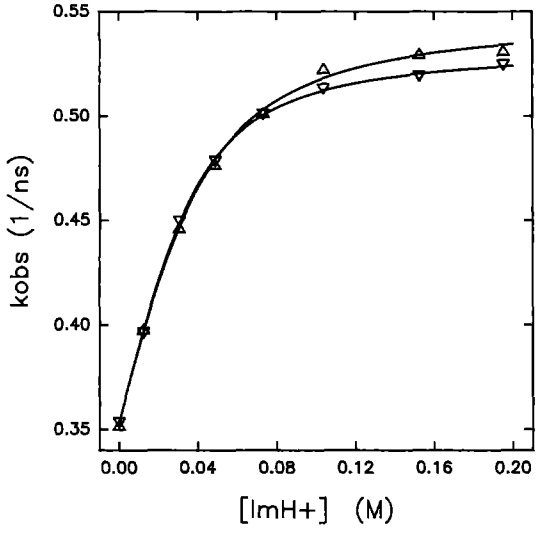

Fig. 2. Inverse life-time (kobs) of NATA as a function of the imidazole concentration at pH 4.5, (△−△) with $I = 0.34$ and (▽−▽) $I = 0.5$. The continuous line is the fitted curve using (9). The parameters obtained are shown in Table 1

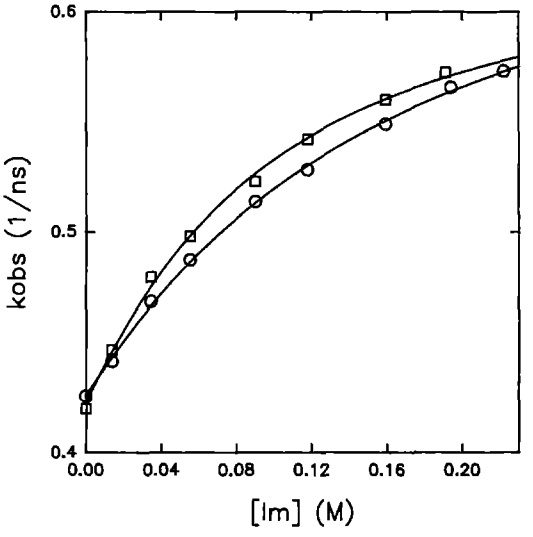

Fig. 3. Titration of NATA with Imidazole at pH 9.0 (○−○) with $I = 0.34$ and (□−□) at $I = 0.5$. The continuous line is the fitted curve using (9). The parameters obtained are shown in Table 1

equilibration:

$$d[T^*]/dt = -k_0[T^*] - k_1[Im][T^*] + k_{-1}[T^* \cdot Im] \quad (4)$$

$$d[T^* \cdot Im]/dt = -k_2[T^* \cdot Im] + k_1[Im][T^*] - k_{-1}[T^* \cdot Im]. \quad (5)$$

Since the fluorescence of both states is always measured together, the two equations can be summed. This leads to (6):

$$d\{[T^*] + [T^* \cdot Im]\}/dt = -k_0[T^*] - k_2[T^* \cdot Im]. \quad (6)$$

Depending on the relative values of the rate constants three situations can be envisaged:

1) A fast equilibrium between the two excited states

Assuming that T^* and $T^* \cdot Im$ are in fast equilibrium with each other with equilibrium constant K:

$$K = [T^* \cdot Im]/[T^*] \cdot [Im]$$

equation (6) can be rewritten:

$$d\{[T^*] + [T^* \cdot Im]\}/dt = -\{[T^*] + [T^* \cdot Im]\} \frac{\{k_0 + k_2 \cdot K \cdot [Im]\}}{(1 + K \cdot [Im])} \quad (7)$$

Table 1. The parameters (upper number) and their standard deviation (lower number) obtained by fitting the data of Figs. 2 and 3 to (8) i.e. k_0, k_2 and K (except those marked *). The same data were fitted with (9) giving parameters k_0, k_2, k_1 and k_{-1}. * The phase data at high viscosity are analysed differently. Two fluorescence life-times could be resolved when the amplitude fractions were of comparable magnitude. At the extremes of the imidazole concentrations, resolution is more difficult. Therefore the phase data were fitted to a single (average) life-time and k_0 and k_2 were obtained as before. All the phase data were then fitted to a sum of two exponentials with these two rate constants and the best fitting amplitudes (and steady state fractions) were calculated. The equilibrium constant K is obtained from fitting the steady state fraction of the longest life-time to (10). ** Fitting to (9) gives a well defined k_1/k_{-1} but ill defined individual parameters diagnostic of a high k_{-1} value. Therefore the fitting was repeated with $k_1 = 5.0 \times 10^9\ M^{-1}\ s^{-1}$ and the other parameters free. In this way it is assumed that the rate constant for diffusional encounter is the same at high and low pH

	pH 4.5 I 0.5	pH 4.5 I 0.34	pH 4.5 I 0.34 50% gly	pH 9.0 I 0.1	pH 9.0 I 0.34
k_0 (ns^{-1})	0.349	0.349	0.278	0.425	0.422
	0.006	0.006	0.002	0.001	0.003
k_2 (ns^{-1})	0.560	0.576	0.682	0.704	0.682
	0.009	0.009	0.016	0.010	0.013
K (M^{-1})	29.8	25.8	10.2*	5.12	7.39
	4.9	3.7	0.1	0.37	0.88
k_0 (ns^{-1})	0.353	0.353		0.425	0.422
	0.001	0.003		0.002	0.002
k_2 (ns^{-1})	0.534	0.549		0.677	0.639
	0.002	0.006		0.010	0.011
k_1 ($M^{-1}\ ns^{-1}$)	4.85	5.16		5.0	5.0
	0.36	1.12		**	**
k_{-1} (ns^{-1})	0.047	0.073		0.67	0.37
	0.009	0.035		0.06	0.05

giving an observed decay constant k_{obs}:

$$k_{obs} = \frac{\{k_0 + k_2 \cdot K \cdot [Im]\}}{(1 + K \cdot [Im])}. \tag{8}$$

Using this equation, a very good fit to the data could be obtained by non-linear least squares fitting using SigmaPlot®. The parameters obtained and their errors are given in Table 1.

2) Coupled excited-state reactions

A set of coupled differential equations (such as 4 and 5) has been solved very generally (e.g. Bernasconi 1976, p. 26) and leads to two rate constants $\lambda\pm$ = eigenvalues):

$$\lambda\pm = \Sigma \pm \sqrt{\Sigma^2 - k_2 k_1 [Im] - k_0 (k_2 + k_{-1})} \tag{9a}$$

with

$$\Sigma = (k_0 + k_1 \cdot [Im] + k_2 + k_{-1})/2 \tag{9b}$$

Although two decay constants ($\lambda\pm$) are predicted, we only observed one. A perfect fit could be obtained with the smallest rate constant ($\lambda-$). We therefore assume that the highest rate constant ($\lambda+$) has a small amplitude which makes it difficult to determine by phase fluorometry. (A simulation of a double exponential decay with $\lambda-$ and $\lambda+$ as rate constants, equal amplitudes, and added experimental noise was made. Analysis by our program showed that the recovery of the two rate constants was possible in these conditions). The results of the fitting are shown in Figs. 2 and 3 and the parameters are found in Table 1.

3) Excited state heterogeneity

If the equilibration of the association equilibrium is slow compared to the fluorescence decay rates, (4) and (5) are limited to their first terms, and lead to a fluorescence decay described by a sum of two exponentials with k_0 and k_2 as rate constants. The ratio of $[T]$ to $[T \cdot Im]$ is controlled by the ground state equilibrium constant. The same is true for the initial concentrations of the excited states and consequently for the steady state amplitudes.

$$[T^*]/([T^*] + [T^* \cdot Im]) = [T]/([T] + [T \cdot Im])$$
$$= 1/(1 + K \cdot [Im]) \tag{10}$$

This situation is approached here by adding 50% (w/w) of glycerol to increase the viscosity to 5 cp. Here indeed the fitting of the phase data can be strongly improved by using two life-times. The results of the phase measurements at pH 4.5, $I = 0.34$, 0.05 M imidazolium at high viscosity are shown in Fig. 4 and the two life-times are given. The resolution at more extreme amplitude ratios is more difficult. Therefore the weighted average life-time is calculated at each imidazole concentration by fitting to a single life-time. These results show again a hyperbolic behaviour. With the two extreme inverse life-times calculated from this curve, the amplitude and steady state fractions are calculated at the different imidazole concentrations. The imidazole-concentration dependence of the steady state fraction of the longest life-time is shown in Fig. 5 and the fitting to (10) gives the association constant found in Table 1.

The two methods of analysis give an almost perfect agreement for k_0, and k_2. It should be noted that the ratio $k_0/k_2 = 0.61\ (\pm 0.01)$ for all the measurements, except at high glycerol concentration, where it is 0.407. This indicates that, with the mentioned exception, the same mechanism is operative at both pH values. The effect of different ionic strength is very limited.

The value for k_1 obtained at low pH is about $5\ (\pm 0.2) \times 10^9\ M^{-1}\ s^{-1}$, which is very close to the theoretical maximal value of $9 \times 10^9\ M^{-1}\ s^{-1}$ at 25 °C and in water.

The fitting of the data at high pH with (9) gives rise to ill defined values of k_1 and k_{-1}, although their ratio is well defined. (This is indicative of a high k_{-1} value, see further). We therefore constrained the fitting procedure with $k_1 = 5.0 \times 10^9\ M^{-1}\ s^{-1}$, which seems reasonable since there is no reason why association should not be diffusion controlled at high pH as it is at low pH.

Despite the similar quality of the fitting by both equations, the equilibrium constants K_1 obtained by (9) are between 3.4 (low pH) and 1.4 (high pH) times higher than the constant K obtained from fitting to (8). This can be easily understood since it can be shown from the deriva-

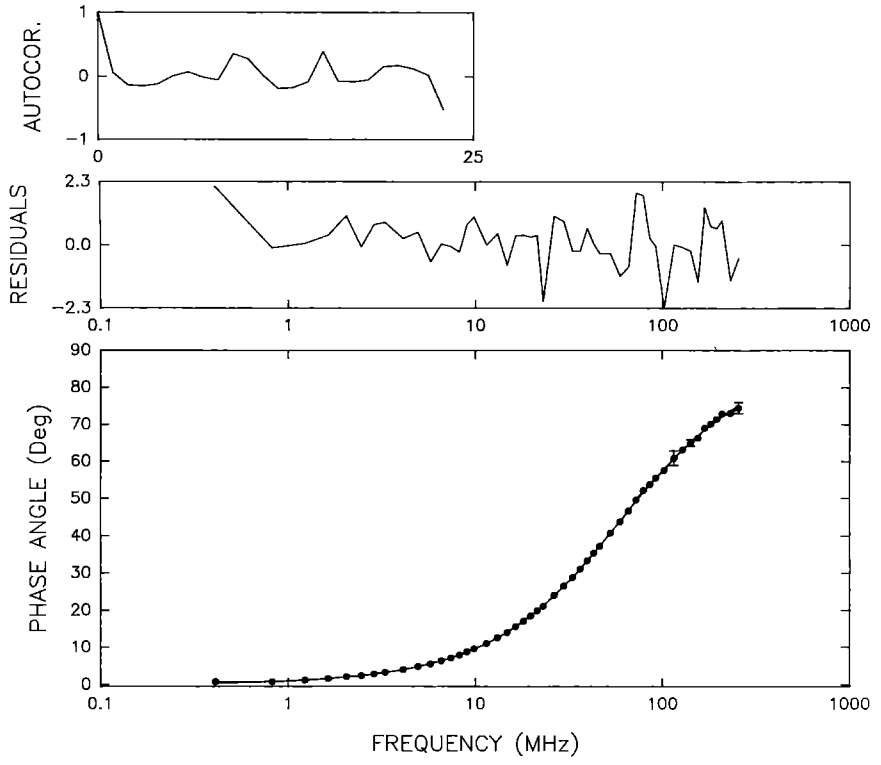

Fig. 4. Phase measurements of NATA at 0.05 M imidazole, pH = 4.5, $I = 0.34$ M and 50% (w/w) glycerol. Plotted are the measured phases and weighted residuals as a function of the frequency and the autocorrelation function of the weighted residuals. The fitting and quality of fit parameters are: reduced chi-square $\chi^2_R = 0.842$; the standard normally distributed $Z_\chi 2 = -1.908$; quality parameter $Q = 0.88$. Two life-times are observed: $\tau_1 = 2.9225 \pm 0.050$ ns amplitude fraction $= 0.56 \pm 0.11$, $\tau_2 = 1.484 \pm 0.15$ ns

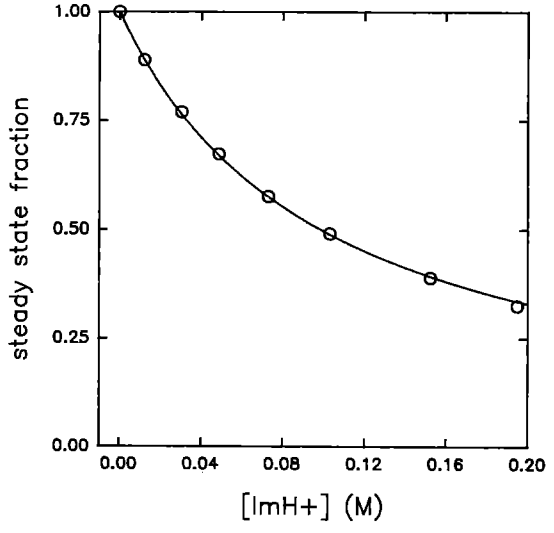

Fig. 5. Analysis of the phase measurements at high viscosity. The steady state fraction of the longest life-time is plotted versus imidazolium concentration. The data are fitted with a simple binding function: steady state fraction $= 1/(1 + K \cdot [ImH^+])$. The value obtained for K is 10.2 ± 0.1 M^{-1}

tives of (8) and (9) in the origin, that

$$\{d(\lambda -)/d[Im]\}_{[Im]=0} = k_1(k_2 - k_0)/(k_2 - k_0 + k_{-1}) \quad (11)$$

$$\{dk_{obs}/d[Im]\}_{[Im]=0} = K(k_2 - k_0) \quad (12)$$

$$K = k_1/(k_2 - k_0 + k_{-1}) \quad (13)$$

i.e. K is comparable to a Michaelis-Menten constant. These equations also prove that when k_{-1} is high, only the ratio k_1/k_{-1} is determined.

The values of the association equilibrium constant of the first step (K_1) are much higher than the value (0.4 M^{-1}) calculated for a collisional complex between imidazole (radius = 2.1 Å) and tryptophan (radius = 3.3 Å) (Strehlow and Knoche 1977). Stacking of the two ring systems could be the reason for this affinity. Furthermore it is clear that complex formation in acid medium is much stronger than in basic medium, possibly due to additional H-bridges, induced dipole or charge transfer effects by the protonated imidazole.

The effect of glycerol is to slow down the association equilibrium giving rise to an heterogeneous system with two well definable life-times. An effect of glycerol as solvent on the fluorescence process itself is apparent in slightly different k_0 and k_2 values and their different ratio. The stability of the initial complex, as calculated from the concentration dependence of the amplitude ratio, is about 7 times smaller than its value (K_1) in the same conditions without glycerol. This proves that glycerol slows down the association and dissociation rate constants to a different extent.

The different life-times obtained for *Trp* in contrast to the single life-time for NATA prove the importance of the presence of charged groups in the immediate neighbourhood of the indole ring (Szabo and Rayner 1980a, b). While NATA is the best model for a *Trp* residue in a protein, the side chains of the other amino acids may provide quenching interactions. When the fluorescence of the three *Trp* protein barnase and its mutants (Loewenthal et al. 1991; Willaert et al. 1991) was studied another important side chain was encountered: the imidazole ring. *Trp*-94 is strongly quenched by this group in a pH-dependent way, with the most pronounced effect at low pH. It is therefore rather surprising to see that in the solution study the ratio of the fluorescence life-time of the complex to the life-time of free tryptophan (0.61 ± 0.01), is independent of pH. Nevertheless the protonated form is a better quencher because the complex has a longer resi-

dence-time (lower k_{-1}) and therefore has a greater chance to emit from the complexed state.

The higher efficiency of quenching at low pH in barnase indicates that either;

(*i*) another mechanism is responsible for the quenching. Although the fluorescence follows exactly the *pka* of *His*-18, it should be noted that the orientation of the two side chains in barnase is almost certainly different from the situation in solution.

(*ii*) the dynamics of the protein also allow for the establishment of a kind of association-dissociation equilibrium, with a more pronounced association in the protonated state of *His*-18. A molecular dynamics trajectory (with unprotonated imidazole) proves the frequent contact between the side chain atoms of the two residues (Van Belle et al. 1985). Such a phenomenon may also lead to life-time heterogeneity: if the protein allows for two more slowly interconverting conformational states with a sufficient change in the *Trp-His* distance, two life-times could develop.

The present empirical approach demonstrates that the effect of imidazole is not just a simple collisional quenching, but a facilitation of the fluorescence decay by complex formation. We hope that these results will allow the theoretical photophysicists to deduce the nature of the mechanism that leads to the reduced life-time.

The results obtained here suggest the possibility to study other side chain groups of amino acids as possible quenchers for *Trp* fluorescence. Possible candidates are the negative charges of Glu and Asp and the positive charges of Lys, Arg, and the heavy $-SH$ groups. The importance of these groups, including the imidazole group, was suggested by Bushueva et al. (1974, 1975) on the basis of steady state fluorescence measurements but no life-time studies were performed.

In papain, related proteins and some small peptides a correlation was observed between the steady state fluorescence and the ionization of an His residue by Shinitzky and Goldman (1967).

Acknowledgements. This work is supported by the Belgian State Prime Minister's Office Science Policy Programming. K.W. was supported by this program and by the I.W.O.N.L. Y.E. is research director of the Belgian National Fund for Scientific Research.

References

Bernasconi CF (1976) Relaxation kinetics. Academic Press, New York San Francisco London

Bevington PB (1969) Data reduction and error analysis for physical sciences, McGraw-Hill, New York

Bushueva TL, Busel EP, Bushuev VN, Burstein EA (1974) The interaction of protein functional groups with indole chromophore. I. Imidazole group. Studia Biophys 44:129–139

Bushueva TL, Busel EP, Burstein EA (1975) The interaction of protein functional groups with indole chromophore. III. Amine, amide and thiol groups. Studia Biophys 52:41–52

Clays K, Jannes J, Engelborghs Y, Persoons A (1989) Instrumental and analysis improvements in multifrequency phase fluorometry. J Phys E: Sci Instrum 22:297–305

Desie G, Boens N, De Schrijver FC (1986) Study of the time-resolved tryptophan fluorescence of crystalline α-chymotrypsin. Biochemistry 25:8301–8308

Loewenthal R, Sancho J, Fersht A (1991) The fluorescence spectrum of barnase: contributions of three tryptophan residues and a histidine-related pH-dependence Biochemistry 30:6775–6779

More JJ, Sorensen DC (1983) Computing a trust region step. SIAM J Sci Stat Comp 4:553–572

Shinitzky M, Goldman R (1967) Fluorometric detection of histidine-tryptophan complexes in peptides and proteins. Eur J Biochem 3:139–144

Strehlow H, Knoche W (1977) Fundamentals of chemical relaxation, Verlag Chemie, Weinheim New York

Szabo AG, Rayner DM (1980) Fluorescence decay of tryptophan conformers in aqueous solutions. J Am Chem Soc 102:554–563

Szabo AG, Rayner DM (1980) The time resolved emission spectra of peptide conformers by pulsed laser excitation, Biochem Biophys Res Commun 94:909–915

Van Belle D, Prevost M, Wodak SJ (1989) Electrostatic properties of solvated proteins: a microscopic analysis based on computer simulation. Chem Scr 29A:181–189

Waldman ADB, Clarke AR, Wigley DB, Hart KW, Chia WN, Barstow D, Atkinson T, Munro I, Holbrook JJ (1987) The use of site-directed mutagenesis and time-resolved fluorescence spectroscopy to assign the fluorescence contributions of individual tryptophan residues in *Bacillus stearother-mophilus* lactate dehydrogenase. Biochim Biophys Acta 913:66–71

Willaert K, Loewenthal R, Sancho J, Froeyen M, Fersht A, Engelborghs Y (1991) Determination of the excited state life-times of the tryptophan residues in barnase, via multifrequency phase fluorometry of tryptophan mutants Biochemistry (submitted for publication)